

Published in final edited form as:

*J Biomed Mater Res A*. 2013 April ; 101(4): 1184–1194. doi:10.1002/jbm.a.34412.

## Biochemically and topographically engineered poly(ethylene glycol) diacrylate hydrogels with biomimetic characteristics as substrates for human corneal epithelial cells

B. Yañez-Soto<sup>1</sup>, S.J. Liliensiek<sup>1</sup>, C. J. Murphy<sup>2,3</sup>, and P. F. Nealey<sup>1,\*</sup>

<sup>1</sup>Department of Chemical and Biological Engineering, School of Engineering, University of Wisconsin, Madison, 53706, WI, USA

<sup>2</sup>Department of Veterinary Surgical and Radiological Sciences, School of Veterinary Medicine, University of California, Davis, Davis, CA, 95616, USA

<sup>3</sup>Department of Ophthalmology and Vision Sciences, School of Medicine, University of California, Davis, Davis, CA, 95817, USA

### Abstract

Incorporation of biophysical and biochemical cues into the design of biomaterials is an important strategy for tissue engineering, the design of biomedical implants and cell culture. Hydrogels synthesized from poly (ethylene glycol) diacrylate (PEGDA) were investigated as a platform to simultaneously present human corneal epithelial cells (HCECs) *in vitro* with topography and adhesion peptides to mimic the native physical and chemical attributes of the basement membrane underlying the epithelium *in vivo*. Hydrogels synthesized from aqueous solutions of 20% PEGDA (MW of 3400 g/mol) prevented non-specific cell adhesion and were functionalized with the integrin-binding peptide Arg-Gly-Asp (RGD) in concentrations from 5 to 20 mM. The hydrogels swelled minimally after curing and were molded with ridge and groove features with lateral dimensions from 200 nm to 2000 nm and 300 nm depth. HCECs were cultured on topographic surfaces functionalized with RGD and compared to control unfunctionalized topographic substrates. HCEC alignment, either parallel or perpendicular to ridges, was influenced by the culture media on substrates promoting non-specific attachment. In contrast, the alignment of HCECs cultured on RGD hydrogels showed substantially less dependence on the culture media. In the latter case, the moldable RGD-functionalized hydrogels allowed for decoupling the cues from surface chemistry, soluble factors, and topography that simultaneously impact HCEC behavior.

### Keywords

Biomimetic material; epithelial cell; hydrogel; polyethylene glycol; nanotopography

### Introduction

Transplantation with human donor corneal grafts is the primary treatment for the majority of corneal disorders that cause visual impairment<sup>1</sup>. However, demand for grafts far exceeds the amount of donor tissue available and the success rate of corneal transplantation with human donor tissue is reduced in patients with certain pathologies<sup>2</sup>, emphasizing the need for artificial prostheses<sup>3</sup>. We hypothesize that the incorporation of both biochemical (molecules interacting with the cell) and biophysical (topography and compliance) cues<sup>4</sup> derived from

\*Corresponding author: Paul F. Nealey, Department of Chemical and Biological Engineering, School of Engineering, 3020 Engineering Hall, 1415 Engineering Drive, Madison, WI, 53706, Phone: (608) 265-8171, nealey@engr.wisc.edu.

the corneal basement membrane (BM), into the surface of artificial corneas may promote human corneal epithelial cell (HCEC) behaviors that support re-epithelialization and tissue regeneration, minimizing complications such as extrusion, infection and epithelial down-growth<sup>2,5</sup> of current corneal prostheses.

Previous research from our laboratory has quantified the topography of the corneal BM<sup>6</sup>, and demonstrated that the scale of the topography modulates adhesion<sup>7</sup>, contact guidance<sup>8,9</sup>, migration<sup>10</sup> and proliferation<sup>11</sup> in HCECs. In addition, HCECs cultured in serum-free media exhibited alterations in the response to topographic cues when the features transitioned between the nano and micron scale, such as cells aligning parallel to microscale ridges, but perpendicular to nanoscale ridges<sup>8,12-14</sup>. These results demonstrate that topographic cues of relevant nano and submicron size should be considered and incorporated in the design criterion for a synthetic BM, and suggest the synergistic influence of several factors including topographic cues, the adsorbed protein layer, and soluble factors. However, the nonspecific adsorption of proteins on the rigid substrates utilized in these experiments precludes specific knowledge of the surface chemistry, thereby complicating the potential isolation of the specific cell substrate receptors involved in the response to biophysical cues and the identification of downstream signaling pathways responsible for the differential cell behaviors observed. A major objective of our study is the development of soft substrates with controlled surface chemistry that allow for the inhibition of non-specific protein adsorption, the provision of well-defined cell-substrate adhesion motifs, and the simulation of the *in vivo* range of topography<sup>15</sup>.

Poly(ethylene glycol) (PEG) hydrogels are excellent candidates as biomaterials because of their potential for incorporating both biophysical and biochemical cues and their prevention of non-specific protein adsorption, biocompatibility and FDA approval for use in humans<sup>16,17</sup>. PEG hydrogels can be synthesized using a variety of established methods that allow for integration of ligands<sup>18</sup> or co-polymerization with biodegradable materials<sup>19,20</sup>. In addition, topographic micron-scale features have been incorporated into UV-polymerizable hydrogels using soft lithography<sup>21</sup> and photolithography<sup>22</sup>.

The peptide RGD (Arg-Gly-Asp) is a rational first choice as the bioactive ligand to be incorporated into PEG hydrogels to provide specific and relevant adhesion moieties to the HCECs because this sequence is involved in binding to cell substrate adhesion receptors including several integrins<sup>23</sup>. In the cornea, the epithelial basal cells are in direct contact with the BM and exhibit high expression levels of the RGD-binding  $\alpha_5\beta_1$  integrin<sup>24</sup>, while corneal epithelial cells migrating across a wound express  $\alpha_5\beta_1$  integrin at increased levels<sup>25,26</sup>. In wound healing experiments *in vitro* using HCECs, the wound closure rate increased from 2  $\mu\text{m}/\text{h}$  in the absence of RGD up to 10  $\mu\text{m}/\text{h}$  with 80% RGD content<sup>27</sup>. In aggregate, these studies support the use of RGD as a peptide to elicit specific adhesion responses in HCECs and decouple the influence of surface biochemistry and topography on HCEC response.

Herein, we report the fabrication of PEGDA substrates that allow for the simultaneous presentation of uniform biochemistry and biotopography to HCECs. The purpose is to investigate whether the scale of topography on substrates with controlled mechanisms of cell attachment differentially modulates cell behavior in the presence or absence of other cues, including external soluble factors from the media. The results from this study are important to our understanding of HCEC behavior in the presence of multiple cues and will aid in the development of more biologically and clinically relevant materials and systems.

## Materials and methods

### Synthesis of PEG diacrylate (PEGDA)

PEGDA pre-polymers of molecular weight 3400 g/mol (PEGDA 3400) and 8000 g/mol (PEGDA 8000) were synthesized according to previously published methods<sup>28</sup>. Briefly, PEGDA was synthesized by combining 3 grams of vacuum-dried OH-terminated PEG (Hampton Research, NJ) into 50 mL of anhydrous toluene (Acros Organics, NJ) with 2X molar excess acryloyl chloride (Sigma-Aldrich, MD) and 2X molar excess triethylamine (Sigma-Aldrich, NJ) with respect to the oligomer end-groups. The mixture was incubated for four hours at 70° C in nitrogen. The resulting insoluble triethylamine salts in the solution were filtered and the PEGDA was precipitated in cold diethyl ether and dried for 48 hours. PEGDA was dialyzed using dialysis tubing for four hours with three changes of Milli-Q H<sub>2</sub>O (Millipore). The lyophilized product was verified with <sup>1</sup>H NMR spectrometry using a Bruker AC-300 instrument and matrix-assisted laser desorption/ionization time-of-flight (MALDI-TOF) mass spectrometry with a Bruker Reflex II instrument.

### Measurement of the swelling ratio in unbound PEGDA hydrogels

Precursor solutions of various mass fractions (Table I) were prepared by dissolving either PEGDA 8000, PEGDA 3400 or PEGDA of molecular weight 700 g/mol (PEGDA 700) (Sigma-Aldrich, Japan) in 10 mM 4-(2-hydroxyethyl)-1-piperazineethanesulfonic acid (HEPES) buffer at pH 8.0. Either 0.05% mass concentration (w/v) 1-propanone, 2-hydroxy-1-[4-(hydroxyethoxy)phenyl]-2-methyl-1-propanone (Irgacure 2959, Ciba AG) or 0.067% w/v Lithium phenyl-2,4,6-trimethylbenzoylphosphinate (LAP) was used as the photoinitiator. A 30 μL drop of the precursor solution was placed on top of a degassed poly(dimethyl siloxane) (PDMS, Sylgard® 184, Dow Corning, MI) surface using a 1 mm spacer in nitrogen atmosphere. The precursor solution was then covered with another PDMS surface. The hydrogels were polymerized under long wavelength UV light (364 nm for 900 s at 7.0 mW/cm<sup>2</sup>) and their weight was measured immediately ( $W_R$ , relaxed gel weight). Gels were then soaked in DI water for 72 hour and their equilibrium swollen weight ( $W_s$ ) was measured after removing excess water by carefully wicking with a spatula. Gels were frozen and lyophilized and their dry weight was measured ( $W_D$ ). The relaxed swelling ratio ( $Q_R$ ) (volume of swollen gel/volume of relaxed gel) was approximated as  $Q_R = [W_{SPol} + W_D(\rho_w - \rho_{Pol})] / [W_{RPol} + W_D(\rho_w - \rho_{Pol})]$ ; where  $\rho_{Pol}$  is the density of PEG (1.1192 g/mL) and  $\rho_w$  is the density of water (0.9982 g/mL) at 20° C.

### Synthesis of ECM peptides

RGD peptide (Cys-Gly-Gly-Arg-Gly-Asp-Ser-Pro) and control scrambled peptide RDG (Cys-Gly-Gly-Arg-Asp-Gly-Ser-Pro) were synthesized by solid phase peptide synthesis on Fmoc-Rink Amide MBHA resin with Fmoc-protected  $\alpha$ -amino groups using a peptide synthesizer (CS Bio, Menlo Park, CA). 2,2,5,7,8-pentamethyl-chroman-6-sulfonyl was used as side-chain protecting group for Arg. The resulting peptide molecules were cleaved from the resin for four hours using a TFA:TIS:water (95:2.5:2.5) solution, filtered to remove resin and precipitated in diethyl ether. Peptides were analyzed by matrix-assisted laser desorption/ionization time of flight (MALDI-TOF) mass spectrometry (Bruker Reflex II time-of-flight mass spectrometer) and used without further purification.

### Fabrication of substrates with topographic features

Precursor solutions of 20% (w/w) PEGDA were prepared by dissolving PEGDA 8000, PEGDA 3400 or PEGDA 700 in 10 mM HEPES buffer at pH 8.0. Either 0.05% (w/v) Irgacure 2959 or 0.067% (w/v) LAP were used as the photoinitiator. Variable amounts of RGD or control RDG peptide were added to the precursor solutions to reach final

concentrations of 0, 1, 5, 10 or 20 mM. Topography was incorporated into the hydrogel substrates using a replica-molding technique (Figure 1)<sup>29</sup>. In a nitrogen atmosphere, a 30  $\mu$ L drop of the precursor solution was placed on top of a degassed PDMS stamp containing the desired topography with 0.5 mm PDMS spacers. The precursor solution was then covered by a glass coverslip previously treated with 3-(trichlorosilyl) propyl methacrylate (TPM, Sigma-Aldrich, UK) to ensure adhesion of the gels to the surface. The construct was polymerized under UV-light (364 nm for 900 s at 7.0 mW/cm<sup>2</sup>) and the PDMS stamps were peeled off, transferring the pattern to the surface of the hydrogel. Hydrogel substrates were sterilized for 24 hours by soaking in 5% isopropyl alcohol (IPA) in 1X phosphate buffered saline (PBS, pH 7.2), rinsed for 24 hours in 1X PBS and pre-incubated for two hours in the appropriate cell culture media for full equilibration.

For control substrates allowing non-specific protein adsorption, we molded a photocrosslinkable mercapto-ester, Norland Optical Adhesive 81 (NOA-81, Norland Products Inc, NJ) as described previously<sup>11</sup>. The substrates were sterilized for 24 hours in 5% IPA in 1X PBS (pH 7.2), rinsed for 24 hours in 1X PBS and pre-incubated for two hours in the appropriate cell culture media.

### AFM imaging of molded hydrogels

Molded hydrogels containing topographic features were imaged by atomic force microscopy (AFM), using a Nanoscope IIIa Multimode scanning probe microscope (Veeco Instruments Inc., CA). After hydration in PBS for at least 48 h at room temperature, samples were scanned in a fluid cell in contact mode using a SNL-10 silicon nitride cantilever with a silicon tip (Veeco Probes, CA).

### HCEC culture

HCECs were harvested from human cadaver corneas graciously provided by the Lions Eye Bank of Wisconsin, Madison or the Missouri Lions Eye Bank (Columbia, MO) as previously reported<sup>8</sup>. Cells from two to four corneas were centrifuged and re-suspended in either epithelial medium (EP medium)<sup>30,31</sup> or in Epilife® medium (Invitrogen, CA) with a proprietary growth supplement (Epilife® Defined Growth Supplement)<sup>12</sup>. All HCECs were incubated at 37 °C and 5% CO<sub>2</sub> until they reached approximately 70% confluence. HCECs were used between passages 1 and 4.

### Analysis of cell attachment

An experimental set consisted of at least three replicates of each hydrogel substrate plated at a density of 10,000 cells/cm<sup>2</sup>. Cells were incubated for 24 h after plating to allow for attachment and spreading. For the initial cell attachment experiments, cells were washed and the number of remaining HCECs was counted after 24 hours in culture. Hydrogel samples with HCECs were imaged in phase contrast mode using a Zeiss Axiovert 100M fluorescence microscope (Zeiss, NY) with a 10X objective lens. At least four images, encompassing the majority of the hydrogel surface, were taken for each substrate as well as control TCPS. Each experiment was repeated in triplicate.

### Immunocytochemistry

Cells were stained for actin-filaments and nucleus for the measurement of cell number as previously described<sup>14</sup>. Briefly, following incubation, cells were fixed with a 1% paraformaldehyde solution in PBS (Electron Microscopy Sciences, PA) at room temperature for 20 minutes. Cells were then permeabilized with 0.1% (w/v) Triton X-100 (Sigma–Aldrich, MO) in 1X PBS for 7 minutes, and then exposed to 1% (w/v) bovine serum albumin (Sigma–Aldrich, MO) in 1X PBS for 20 min to block non-specific binding. Cells

were then incubated with 5  $\mu\text{g/mL}$  of TRITC-phalloidin (Sigma-Aldrich, MO) containing 0.1  $\mu\text{g/mL}$  4',6-Diamidino-2-phenylindole (DAPI) (Invitrogen, CA) in 1X PBS for 40 minutes, to label both filamentous actin (red), and the nucleus (blue).

### Analysis of cell elongation and alignment

Each experimental set consisted of groups encompassing three types of substrates: substrates made with 10 mM RGD-hydrogel, substrates made with 10 mM scrambled RDG-hydrogel as a negative control, and substrates made with NOA-81 as a fouling control. Each group contained 3–5 samples. The substrates were molded with topographic features containing six separate areas with different ridge/groove widths (400, 800, 1200, 1600, 2000, 4000 nm pitch) and intervening planar control areas<sup>13</sup>. HCECs were plated at a density of 10,000 cells/cm<sup>2</sup> in either EP medium or Eplife®, cultured for 24 hours, fixed and stained. Images of fluorescent cells on each substrate were obtained using a 10X objective lens. On each topographic substrate at least four images were taken of each pitch size and flat control areas present between patterned areas. Image analysis was performed using AxioVision software (Zeiss, NY). The cell elongation and angle of alignment were collected from the images and sorted using parameters previously described by our group<sup>8,32</sup>. Cells were deemed elongated with elongation factors greater than 1.3 and calculated as previously described.<sup>9</sup> A cell was considered aligned parallel if the angle was less than 10° and perpendicular if the angle was between 80° and 90°. Results represent the arithmetic mean percentage of the aligned cells with respect to the total population. Each experiment was repeated in triplicate.

### Statistics

Experimental data were analyzed using analysis of variance (ANOVA). When variability was determined to be significant ( $\alpha=0.05$ ) the Bonferroni multiple comparison test was used to determine significance between flat surfaces and topographic surfaces. Significant results were further divided into “statistically significant” (0.01  $P$  0.05, \*), “very significant” (0.001  $P$  < 0.01, \*\*), and “extremely significant” ( $P$  < 0.001, \*\*\*).

## Results

### Hydrogels synthesized with 20% (w/w) PEGDA 3400 prevent non-specific cell adhesion and retain nanoscale topography

Hydrogels were synthesized through the free radical polymerization of PEGDA using photoinitiators (Scheme 1). The general technique used to mold topographic features into PEGDA hydrogels is depicted in Figure 1. A PDMS substrate containing the topography (Figure 1A) is covered with a spacer and a drop of the precursor solution is placed on top (Figure 1B). The precursor solution is covered with a glass coverslip previously treated with TPM to ensure attachment of the gel to the glass surface (Figure 1C). The hydrogel is UV-photopolymerized and the PDMS stamp is removed (Figure 1D). The hydrogel is then soaked in the proper media (Figure 1F).

To test the retention of the topographic features after swelling of the hydrogels, we first characterized the swelling behavior of hydrogels as a function of molecular weight and concentration, using different precursor solutions (Table I). Free floating hydrogels were synthesized, using the technique depicted in Figure 1 and substituting the glass coverslip with a flat PDMS surface to ensure detachment of the hydrogels. These unbound hydrogels were immediately weighed, soaked in distilled water until equilibration, and subsequently weighed in the fully swollen state. The relaxed swelling ratio ( $Q_R$ ), defined as the ratio of the volume at equilibrium swelling to the volume at the relaxed state (after crosslinking, but before swelling), was calculated as described in the methods section. Figure 2A shows  $Q_R$  as a function of the concentration and molecular weight of precursors. Hydrogels synthesized



using PEGDA 8000 exhibited the highest  $Q_R$ , ranging from 1.6 in P-8000/10 to 2.4 in P-8000/25. Hydrogels made with PEGDA 3400 had a  $Q_R$  ranging from 1 in P-3400/10 to 1.4 in P-3400/25. PEGDA 700 hydrogels demonstrated low levels of swelling over the range of concentrations tested. In summary: 1) swelling increased monotonically with increasing molecular weight of PEGDA, and 2) swelling increased with increasing concentration of the pre-polymer in the mixture.

To test the retention of topographic features after equilibrium swelling, hydrogels containing 4000 nm pitch groove-and-ridges topography were synthesized following the general technique shown in Figure 1. In spite of the low level of swelling obtained with low polymer concentrations, hydrogels made with less than 20% (w/w) polymer failed to replicate the topographic features (results not shown). Therefore, we selected the 20% (w/w) hydrogels to image using atomic force microscopy (AFM). The distortion of topographic features after swelling increased with increasing molecular weight. The features on hydrogels molded using P-8000/20 no longer exhibit sharp edges and have a rounded appearance (see insert in Figure 2A). Due to the large distortion of the topography, PEGDA 8000 was not used in cell culture studies. In the same figure, hydrogels P-700/20 and P-3400/20 can be appreciated to retain the molded features, thus meeting the design objective criteria.

The inhibition of non-specific HCEC attachment was also dependent on the molecular weight of the PEGDA pre-polymer. We tested the non-fouling properties of the hydrogels that demonstrated retention of the topographic features: P-700/20 and P-3400/20. Hydrogels with flat surfaces were synthesized using the technique shown in Figure 1, with flat PDMS molds. HCECs were cultured on the surfaces, and the number of adherent cells was quantified. Although the total cell number on substrates was low, HCECs cultured on P-700/20 hydrogels demonstrated a 2.6-fold increase in cell attachment compared to P-3400/20 (Figure 2B). Hydrogels made with P-3400/20 provided the best balance of non-fouling properties and retention of topographic features and were selected for the experiments functionalizing hydrogels with specific peptides.

### HCECs exhibit specific RGD-dependent attachment on flat functionalized PEG surfaces

Peptides were covalently incorporated to the acrylate groups of the PEGDA macromer via a Michael-type addition reaction<sup>33</sup>, where candidate peptides containing thiol groups react with the acrylate groups present in PEGDA to form stable covalent linkages (Scheme 2). To validate HCEC attachment specificity through integrin binding, variable amounts of the peptide RGD or control “scrambled” RDG were added to P-3400/20 precursor solutions to reach the final peptide concentrations of 1, 5, 10 or 20 mM in the solution. Flat hydrogels were synthesized using the procedure depicted in Figure 1. Hydrogels were sterilized and rinsed and soaked in culture medium until equilibration. HCECs were cultured and stained and imaged for the level of cell attachment. As expected, unfunctionalized P-3400/20 hydrogel surfaces or substrates functionalized with the scrambled peptide RDG showed no significant attachment of HCECs for any of the scrambled peptide concentrations (1–20 mM) (images not shown). Images in Figure 3A demonstrate monotonically increasing number of attached HCECs with increasing concentration of RGD in the hydrogels. The cell number of HCECs on 5 mM RGD substrates increased 33-fold compared to the control unfunctionalized hydrogel and 22-fold compared to the 5 mM scrambled peptide. On 10 mM RGD substrates, the HCEC number increased 49-fold compared to the control unfunctionalized hydrogel and 5-fold compared to the hydrogels functionalized with 10 mM scrambled peptide. HCECs on 20 mM RGD substrates exhibited an extremely significant increase of 60-fold compared to the control unfunctionalized hydrogels and 120-fold increase compared with the 20 mM scrambled peptide (Figure 2B). These results demonstrate that our substrates are non-fouling and possess a controlled biochemistry that allows for specific RGD-integrin attachment.

## Controlled chemical and topographic cues impact HCEC area, elongation ratio and contact guidance differentially in serum-containing and serum-free media

To test the influence of topography on the hydrogels, P-3400/20 hydrogels functionalized with 10 mM RGD were synthesized and molded for cell culture experiments. The topographic molds contained 6 separate areas with different ridge/groove widths (400, 800, 1200, 1600, 2000 and 4000 nm pitch), and intervening planar control areas<sup>13</sup>. HCECs were plated onto these substrates, as well as rigid control surfaces made with NOA-81 that allows non-specific cell-surface interactions. HCECs were cultured in EP medium or serum-free Epilife®. The choice of media was motivated by previous work from our group, where different media compositions have induced alterations in the HCECs response to topographic cues<sup>12,13</sup>. After 24 hours, cells were fixed, stained and imaged. As an example of the differences in orientation, elongation and cell area that can be distinguished in HCECs on different substrates and media compositions, we have included images of HCECs on the 4000 nm pitch topography in Figure 4.

We analyzed and compared the area of the HCECs as a function of topographic feature pitch and media type for each type of substrate (NOA-81, RGD or RDG). HCECs plated onto topographically patterned NOA-81 and cultured in Epilife®, had decreased average area, between 57% and 86% compared to the area of cells plated on flat surfaces (Figure 5A). Although there were no significant differences in cell area between flat surfaces and 400 nm topography when cultured on RGD hydrogels in Epilife®, HCECs on 800 nm pitch topographies were 61% smaller than cells on flat surfaces, while cells plated on large-pitch topographies were 120% (1600 nm pitch) and 126% (2000–4000 nm pitch) larger than cells on flat surfaces (Figure 5B). Cells cultured in EP medium did not show a significant difference in area between the flat substrates and the topographic surfaces, regardless of topographic feature dimensions or substrate composition (Figure 5C and 5D). In summary, cells in Epilife® showed more sensitivity to the underlying topographic features with regards to changes in cell area than cells cultured on EP media for both substrate types.

The average elongation ratio was also compared as a function of topography and media type for each substrate. In Epilife®, the average elongation ratio of cells cultured on 1200–4000 nm pitch substrates increased 20% with respect to the elongation ratio of cells on flat surfaces for both NOA-81 surfaces and hydrogels functionalized with RGD (Fig 6A and 6B). In EP medium, cells cultured on small pitches (400–800 nm) on NOA-81 were significantly more elongated than HCECs on flat surfaces, however, the elongation ratio of cells on topographies larger than 1200 nm was not significantly different when compared to planar surfaces (Figure 6C). On RGD hydrogels in EP medium, HCECs on topographic surfaces exhibited no difference in elongation compared to cells cultured on flat surfaces (Figure 6D). In general, the spreading of HCECs depended on the topographic feature size in Epilife®, but demonstrated a less pronounced dependency on topography when cultured in EP media.

HCEC orientation and alignment with the underlying nano and micron scale topography demonstrated the most noticeable difference in behavior between the two medias used. HCECs presented a bimodal distribution, where cells align either parallel or perpendicular to the topographic features. The proportion of cells in each population varied with substrate and media type. Cells in Epilife® presented a significant and preferential perpendicular alignment for both nano and micron-scale topographies on the NOA-81 substrates (Figure 7A). In contrast, when EP medium was used with the NOA-81 substrates, HCECs exhibited an obvious change in the response to the topographic cues. Cells aligned preferentially parallel to the topography for both nano-sized (400–800 nm) and micron-sized (4000 nm), while the distribution was more uniform on the features transitioning from the nano to the micron-scale (1200–1600 nm). On these substrates we can distinguish a “U” shape in the

alignment profile (Figure 7C). HCECs cultured in either EP medium or Epilife® on RGD-hydrogel substrates displayed a parallel alignment profile matching the aforementioned “U” shape (Figures 7B and 7D). In conclusion, contact guidance was dependent on both the substrate type and soluble factors within the culture media.

## Discussion

Non-fouling PEGDA hydrogel substrates were developed to simultaneously present biologically relevant biochemical and topographical cues to cells in a soft material. One important aim of this work was to identify a soft moldable material that allows for the retention of topographic features in the nano and micron-scale, and provides controlled interactions of HCECs with specific ligands. These biomimetic characteristics can be useful to induce cell behaviors that better approximate *in vivo* conditions and will be essential for our future goal of developing an improved corneal prosthetic.

The Michael-type reaction was chosen for the incorporation of biochemistry into our hydrogel because its rapid reaction times and lack of undesirable by-products<sup>33</sup>. This technique is suitable for single molecules at low concentrations and short-time periods, such as those required by our study. For studies requiring longer temporal stability, our group is investigating other functionalization systems, such as the growth polymerization of acrylated peptides with well-defined spacer length where multiple peptides can be used at varied combinations and concentrations without change in the hydrogel properties<sup>34</sup>.

According to our results, low relaxed swelling ratios are required in order to retain the nano and micro-scale topographic features on a hydrogel. The increase of the relaxed swelling at increasing molecular weight of the oligomer is due to the reduced crosslinking density, allowing for greater penetration of solvent. The swelling increased while increasing the concentration of PEGDA because the pre-polymer is already in a solvated state, and the chemical potential of the PEG chains in the gel increases with concentration, leading to the increased penetration of solvent to equilibrate<sup>35</sup>. The molding of topographic features also depends on the crosslinking density of the hydrogels, and at very low concentrations (15%), the hydrogels did not retain the topographic features.

Multifunctional poly(acrylate) (PA) regions generated during the cross-linking of the materials could potentially modify the non-fouling properties of the hydrogels. Studies from Park, et. al.<sup>36</sup> and Nolan, et. al.<sup>37</sup> have indicated potential issues with non-specific binding of several different cell-types to low molecular weight PEGDA hydrogels. Our results were in accord with these previous studies as HCECs attached non-specifically to P-700/20, but not to P-3400/20. The non-specific cell attachment most likely occurs via the generation of multifunctional poly(acrylate) (PA) regions during cross-linking of the materials through free-radical polymerization (Scheme 1)<sup>38,39</sup>. In the formed hydrogels, the ratio of PA domains to PEG domains increases with decreasing molecular weight. PEGDA 700 has a PA:PEG ratio of 15%, while the PA:PEG ratio in PEGDA 3400 is 3%, thereby potentially increasing the level of non-specific binding for the low molecular weight PEGDA<sup>39-41</sup>. In summary, hydrogels made with low molecular weight of PEGDA were dismissed as feasible substrates because of their tendency to allow for non-specific interactions with HCECs.

The direct correlation between cell attachment and concentration of the RGD peptide, and the specificity of the attachment shown in our work is consistent with observations made in other studies. Our study defined a concentration of RGD between 1 and 5 mM RGD where cell attachment increased greatly up to a threshold concentration of 10 mM, where the number of cells attached reaches a plateau. The determined threshold concentration of peptide that promotes adhesion correlates well with other epithelial cell studies. In Mertz, et.



al. a hyaluronic acid scaffold functionalized with 4 mg/mL (2 mM) of RGD induced faster epithelial outgrowth than control surfaces and surfaces with 2 mg/mL peptide (1 mM)<sup>42</sup>. In addition, Epithelial cells demonstrated enhanced spreading when the RGD density was increased from 0.01 mM to 1 mM on PEG hydrogels<sup>43</sup>. Although the cell affinity for RGD peptides is greatly increased by the use of cyclic RGD<sup>44</sup>, the focus on this work was to test our ability to incorporate biochemical molecules to topographic substrates, therefore a short sequence that has demonstrated specific HCEC attachment was used<sup>34</sup>.

The different response in cell area and elongation ratio of HCECs on topographically patterned nano and micron-scaled surfaces when different media is used further demonstrates the effect of cytoactive soluble factors on the cellular response to the topography and suggests that soluble factors control these parameters on the response to topography more than protein adsorption. While HCECs cultured on NOA-81 surfaces showed a completely different response to topography when different media was used, cells cultured on RGD topographic surfaces showed a similar alignment profile, regardless of the media. This suggests that the alignment behavior depends on two non mutually-exclusive components: 1) protein adsorption from the media, which is inhibited on the RGD functionalized PEG surfaces, 2) the presence of surface-bound RGD that has a greater impact in the alignment response and overrides the influence of the soluble factors. In addition, we noted that contact guidance of HCECs on NOA-81 differs from previously reported studies of primary HCECs on silicon substrates<sup>12</sup>. HCECs cultured in Epilife® on NOA-81 surfaces exhibited perpendicular alignment on all topographies while on silicon substrates, cells preferentially aligned perpendicular to the topography below micron-sized features and parallel on features larger than one micrometer. This disparity may be due to a difference in the profile of protein adsorption on silicon compared to NOA-81, or to small differences on the horizontal and vertical scales of the topographic features<sup>12,13</sup>. However, all of our results strengthen the argument that the HCEC response to the topographic cues is controlled by interplay between topographic and soluble cues. The use of our functionalized hydrogel platform allows for discerning between the contribution of topography on cell behavior, and the confounding non-specific protein adsorption effect.

Differences in the media composition could potentially explain the alteration in the response to nano and micron-scale topographic cues. Previous work from our laboratory has demonstrated that the composition of the media regulates the topographic response of HCECs<sup>13</sup>. However, until now, it has been difficult to dissociate the contribution of the proteins adsorbing onto the surface from other soluble factors in the media, but through the use of materials that inhibit protein adsorption yet promote cell attachment through specific receptors, the influence of soluble constituents can be isolated. The alignment behavior of HCECs was substantially less context-dependent when cells were cultured on RGD-functionalized hydrogels, suggesting the influence of protein adsorption on contact guidance for the NOA-81 surfaces. Although there may be some effects from protein adsorption onto the hydrogel surfaces, we specifically selected a material that is resistant to protein adsorption. We believe that the differential response observed in cell area and elongation of HCECs when cultured in different media on RGD-functionalized hydrogel surfaces is due mainly to the effect of soluble cues on the topographic response.

Several differences between the two medias used could potentially explain the alteration in response to nano and micron scale topographic cues<sup>12</sup>: 1) The presence of serum in EP medium, 2) a 10-fold increase in epidermal growth factor (EGF) in EP medium with respect to Epilife®, and 3) a 10-fold increase in soluble Ca<sup>2+</sup> in EP medium. Future studies will elucidate the role of these factors in downstream signaling that lead directly to changes in the orientation response to topography.

In summary, we fabricated non-fouling substrates that are moldable with nanotopography and that can be functionalized with specific biochemical motifs to promote HCEC attachment. Besides RGD, our topographic hydrogel substrates can allow for the incorporation of different adhesive peptides found in fibronectin or laminin that promote the binding and signaling of other receptors, such as syndecans or the  $\alpha_6\beta_4$  integrin, which have been established as key components in corneal epithelial wound healing<sup>45,46</sup>. These substrates have the potential to mimic certain characteristics of the ECM and improve *in vitro* and *in vivo* applications.

## Conclusions

This study demonstrates that soft materials such as PEGDA hydrogels can be used to engineer substrates incorporating relevant cellular cues, such as controlled biochemistry and topography. The choice of PEGDA molecular weight and concentration has to be balanced to minimize the deformation of the topographic features and inhibit non-specific binding. This study provides further evidence that nanoscale topography is a fundamental biomimetic cue impacting cell phenotype, and not only an indirect effect due to the formation of chemical patterns through non-specific protein adsorption. In addition, we successfully isolated the confounding influence of non-specific protein adsorption onto the surfaces from other soluble factors to investigate the effect of nano and microscale topography on HCEC behavior. The use of our hydrogel materials will provide controlled biochemical and topographical cues to HCECs to form an intact epithelial layer and improve corneal prosthetics, and can be used to investigate the behavior of cells *in vitro*.

## Acknowledgments

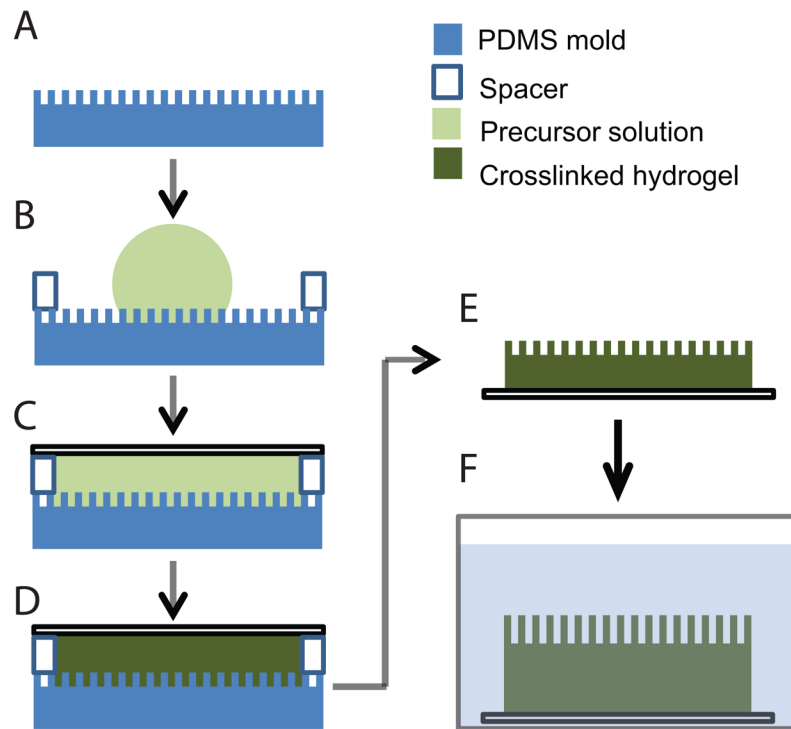
This work is supported in part by NIH-National Eye Institute (1RO1EY017367-01A and 1RO1EY016134-01A2), and by the American Recovery and Reinvestment Act of 2009 through the NIH-National Institute of Arthritis and Musculoskeletal and Skin Diseases (5RC2AR058971-01), and its contents are solely the responsibility of the authors and do not necessarily represent the official views of the National Eye Institute, the National Institute of Arthritis and Musculoskeletal and Skin Diseases or the NIH. The authors wish to thank Michelle Wilson for providing the photoinitiator and technical support in the synthesis of PEGDA, Anna Kiyanova for providing molds and Dr. Nihar Shah for his recommendations and meaningful discussions.

## References

- Whitcher JP, Srinivasan M, Upadhyay MP. Corneal blindness: a global perspective. *Bulletin of the World Health Organization*. 2001; 79:214–221. [PubMed: 11285665]
- Hicks CR, Fitton JH, Chirila TV, Crawford GJ, Constable IJ. Keratoprosthesis: advancing toward a true artificial cornea. *Survey of ophthalmology*. 1997; 42(2):175–189. [PubMed: 9381372]
- Aiken-O'Neill P, Mannis MJ. Summary of corneal transplant activity: Eye Bank Association of America. *Cornea*. 2002; 21(1):1. [PubMed: 11805497]
- Flemming RG, Murphy CJ, Abrams GA, Goodman SL, Nealey PF. Effects of synthetic micro- and nano-structured surfaces on cell behavior. *Biomaterials*. 1999; 20(6):573–588. [PubMed: 10213360]
- Aquavella JV, Qian Y, McCormick GJ, Palakuru JR. Keratoprosthesis: current techniques. *Cornea*. 2006; 25(6):656. [PubMed: 17077656]
- Abrams GA, Schaus SS, Goodman SL, Nealey PF, Murphy CJ. Nanoscale topography of the corneal epithelial basement membrane and Descemet's membrane of the human. *Cornea*. 2000; 19(1):57. [PubMed: 10632010]
- Karuri NW, Liliensiek S, Teixeira AI, Abrams G, Campbell S, Nealey PF, Murphy CJ. Biological length scale topography enhances cell-substratum adhesion of human corneal epithelial cells. *Journal of cell science*. 2004; 117(Pt 15):3153. [PubMed: 15226393]
- Teixeira AI, Abrams GA, Bertics PJ, Murphy CJ, Nealey PF. Epithelial contact guidance on well-defined micro- and nanostructured substrates. *Journal of Cell Science*. 2003; 116(Pt 10):1881–1892. [PubMed: 12692189]

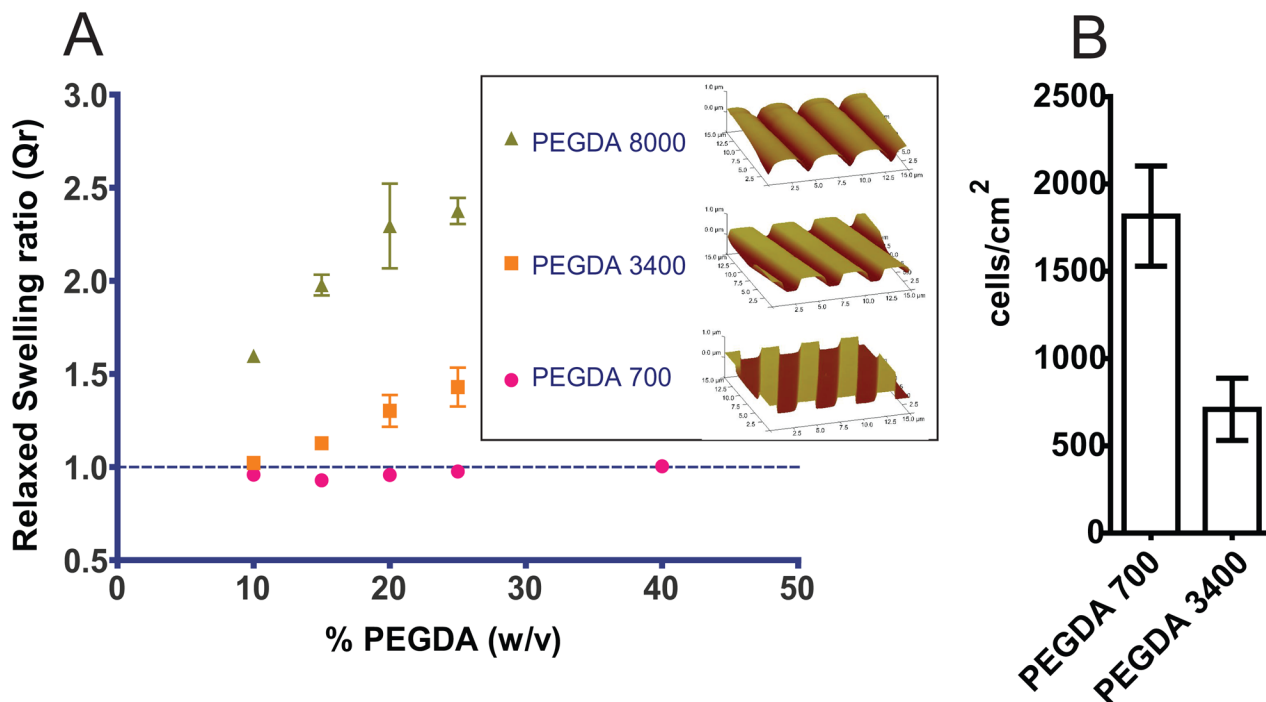
9. Teixeira AI, Abrams GA, Murphy CJ, Nealey PF. Cell behavior on lithographically defined nanostructured substrates. *Journal of Vacuum Science & Technology B: Microelectronics and Nanometer Structures*. 2003; 21:683.
10. Diehl KA, Foley JD, Nealey PF, Murphy CJ. Nanoscale topography modulates corneal epithelial cell migration. *Journal of Biomedical Materials Research Part A*. 2005; 75(3):603–611. [PubMed: 16106433]
11. Liliensiek SJ, Campbell S, Nealey PF, Murphy CJ. The scale of substratum topographic features modulates proliferation of corneal epithelial cells and corneal fibroblasts. *Journal of Biomedical Materials Research Part A*. 2006; 79(1):185–192. [PubMed: 16817223]
12. Teixeira AI, McKie GA, Foley JD, Bertics PJ, Nealey PF, Murphy CJ. The effect of environmental factors on the response of human corneal epithelial cells to nanoscale substrate topography. *Biomaterials*. 2006; 27(21):3945–3954. [PubMed: 16580065]
13. Fraser SA, Ting YH, Mallon KS, Wendt AE, Murphy CJ, Nealey PF. Sub micron and nanoscale feature depth modulates alignment of stromal fibroblasts and corneal epithelial cells in serum rich and serum free media. *Journal of Biomedical Materials Research Part A*. 2008; 86(3):725–735. [PubMed: 18041718]
14. Tocce EJ, Smirnov VK, Kibalov DS, Liliensiek SJ, Murphy CJ, Nealey PF. The ability of corneal epithelial cells to recognize high aspect ratio nanostructures. *Biomaterials*. 2010; 31(14):4064–4072. [PubMed: 20153044]
15. Curtis A, Wilkinson C. Topographical control of cells. *Biomaterials*. 1997; 18(24):1573–1583. [PubMed: 9613804]
16. Lee KY, Mooney DJ. Hydrogels for tissue engineering. *Chem Rev*. 2001; 101(7):1869–1880. [PubMed: 11710233]
17. Drury JL, Mooney DJ. Hydrogels for tissue engineering: scaffold design variables and applications. *Biomaterials*. 2003; 24(24):4337–4351. [PubMed: 12922147]
18. Perlin L, MacNeil S, Rimmer S. Production and performance of biomaterials containing RGD peptides. *Soft Matter*. 2008; 4(12):2331–2349.
19. Metters AT, Anseth KS, Bowman CN. Fundamental studies of a novel, biodegradable PEG-b-PLA hydrogel. *Polymer*. 2000; 41(11):3993–4004.
20. Mann BK, Gobin AS, Tsai AT, Schmedlen RH, West JL. Smooth muscle cell growth in photopolymerized hydrogels with cell adhesive and proteolytically degradable domains: synthetic ECM analogs for tissue engineering. *Biomaterials*. 2001; 22(22):3045–3051. [PubMed: 11575479]
21. Suh KY, Seong J, Khademhosseini A, Laibinis PE, Langer R. A simple soft lithographic route to fabrication of poly (ethylene glycol) microstructures for protein and cell patterning. *Biomaterials*. 2004; 25(3):557–563. [PubMed: 14585705]
22. Revzin A, Russell RJ, Yadavalli VK, Koh WG, Deister C, Hile DD, Mellott MB, Pishko MV. Fabrication of poly (ethylene glycol) hydrogel microstructures using photolithography. *Langmuir*. 2001; 17(18):5440–5447. [PubMed: 12448421]
23. Ruoslahti E. RGD and other recognition sequences for integrins. *Annual review of cell and developmental biology*. 1996; 12(1):697–715.
24. Lauweryns, BvdOJ.; Volpes, R.; Foets, B.; Missotten, L. Distribution of very late activation integrins in the human cornea. *Investigative ophthalmology & visual science*. 1991; 32:2079–2085. [PubMed: 2055701]
25. Jain S, Azar DT. Extracellular matrix and growth factors in corneal wound healing. *Current Opinion in Ophthalmology*. 1994; 5(4):3.
26. Carter RT. The role of integrins in corneal wound healing. *Veterinary Ophthalmology*. 2009; 12:2–9. [PubMed: 19891645]
27. Fong E, Tzllil S, Tirrell DA. Boundary crossing in epithelial wound healing. *Proceedings of the National Academy of Sciences*. 107(45):19302.
28. Lin CC, Metters AT. Metal-chelating affinity hydrogels for sustained protein release. *Journal of Biomedical Materials Research Part A*. 2007; 83(4):954–964. [PubMed: 17580324]
29. Xia Y, Whitesides GM. Soft lithography. *Annual Review of Materials Science*. 1998; 28(1):153–184.

30. Allen-Hoffmann BL, Rheinwald JG. Polycyclic aromatic hydrocarbon mutagenesis of human epidermal keratinocytes in culture. *Proceedings of the National Academy of Sciences of the United States of America*. 1984; 81:7802–7806. [PubMed: 6440145]
31. Sabatini LM, Allen-Hoffmann BL, Warner TF, Azen EA. Serial Cultivation of Epithelial Cells from Human and Macaque Salivary Glands. *In Vitro Cellular & Developmental Biology*. 1991; 27A(12):939–948. [PubMed: 1721908]
32. Teixeira AI, Nealey PF, Murphy CJ. Responses of human keratocytes to micro and nanostructured substrates. *Journal of Biomedical Materials Research Part A*. 2004; 71(3):369–376. [PubMed: 15470741]
33. Elbert DL, Hubbell JA. Conjugate addition reactions combined with free-radical cross-linking for the design of materials for tissue engineering. *Biomacromolecules*. 2001; 2(2):430–441. [PubMed: 11749203]
34. Wilson M, Liliensiek SJ, Murphy CJ, Murphy WL, Nealey PF. Hydrogels with well-defined peptide-hydrogel spacing and concentration: impact on epithelial cell behavior. *Soft Matter*. 2012; 8(2):390–398. [PubMed: 23264803]
35. Bray JC, Merrill EW. Poly (vinyl alcohol) hydrogels. Formation by electron beam irradiation of aqueous solutions and subsequent crystallization. *Journal of Applied Polymer Science*. 1973; 17(12):3779–3794.
36. Park JH, Bae YH. Hydrogels based on poly (ethylene oxide) and poly (tetramethylene oxide) or poly (dimethyl siloxane): synthesis, characterization, in vitro protein adsorption and platelet adhesion. *Biomaterials*. 2002; 23(8):1797–1808. [PubMed: 11950050]
37. Nolan CM, Reyes CD, Debord JD, García AJ, Lyon LA. Phase transition behavior, protein adsorption, and cell adhesion resistance of poly (ethylene glycol) cross-linked microgel particles. *Biomacromolecules*. 2005; 6(4):2032–2039. [PubMed: 16004442]
38. Lin-Gibson S, Jones RL, Washburn NR, Horkay F. Structure- Property Relationships of Photopolymerizable Poly (ethylene glycol) Dimethacrylate Hydrogels. *Macromolecules*. 2005; 38(7):2897–2902.
39. Beamish JA, Zhu J, Kottke-Marchant K, Marchant RE. The effects of monoacrylated poly (ethylene glycol) on the properties of poly (ethylene glycol) diacrylate hydrogels used for tissue engineering. *Journal of Biomedical Materials Research Part A*. 92(2):441–450. [PubMed: 19191313]
40. Kingshott P, Thissen H, Griesser HJ. Effects of cloud-point grafting, chain length, and density of PEG layers on competitive adsorption of ocular proteins. *Biomaterials*. 2002; 23(9):2043–2056. [PubMed: 11996046]
41. Gombotz WR, Guanghui W, Horbett TA, Hoffman AS. Protein adsorption to poly (ethylene oxide) surfaces. *Journal of biomedical materials research*. 1991; 25(12):1547–1562. [PubMed: 1839026]
42. Mertz PM, Davis SC, Franzen L, Uchima FD, Pickett MP, Pierschbacher MD, Polarek JW. Effects of an arginine-glycine-aspartic acid peptide-containing artificial matrix on epithelial migration in vitro and experimental second-degree burn wound healing in vivo. *Journal of Burn Care & Research*. 1996; 17(3):199.
43. Chung IM, Enemchukwu NO, Khaja SD, Murthy N, Mantalaris A, García AJ. Bioadhesive hydrogel microenvironments to modulate epithelial morphogenesis. *Biomaterials*. 2008; 29(17):2637–2645. [PubMed: 18377982]
44. Von Der Mark K, Park J, Bauer S, Schmuki P. Nanoscale engineering of biomimetic surfaces: cues from the extracellular matrix. *Cell and tissue research*. 339(1):131–153. [PubMed: 19898872]
45. Stepp MA, Gibson HE, Gala PH, StaIglesia DD, Pajoohesh-Ganji A, Pal-Ghosh S, Brown M, Aquino C, Schwartz AM, Goldberger O. Defects in keratinocyte activation during wound healing in the syndecan-1-deficient mouse. *Journal of cell science*. 2002; 115(23):4517–4532. [PubMed: 12414997]
46. Jones JCR. The 3 laminin subunit, 6 4 and 3 1 integrin coordinately regulate wound healing in cultured epithelial cells and in the skin. *Journal of Cell Science*. 1999; 112:2615–2629. [PubMed: 10413670]



**Figure 1.** Schematic representation of the technique used to mold PEGDA hydrogels with topographic features: A) Degassed PDMS mold with topographic features. B) A drop of precursor solution is placed on top of the PDMS mold. C) The precursor solution is covered with a glass coverslip previously treated with TPM. D) The hydrogel is UV-polymerized. E) The PDMS mold is removed. F) The hydrogel is soaked until it reaches equilibrium swelling.

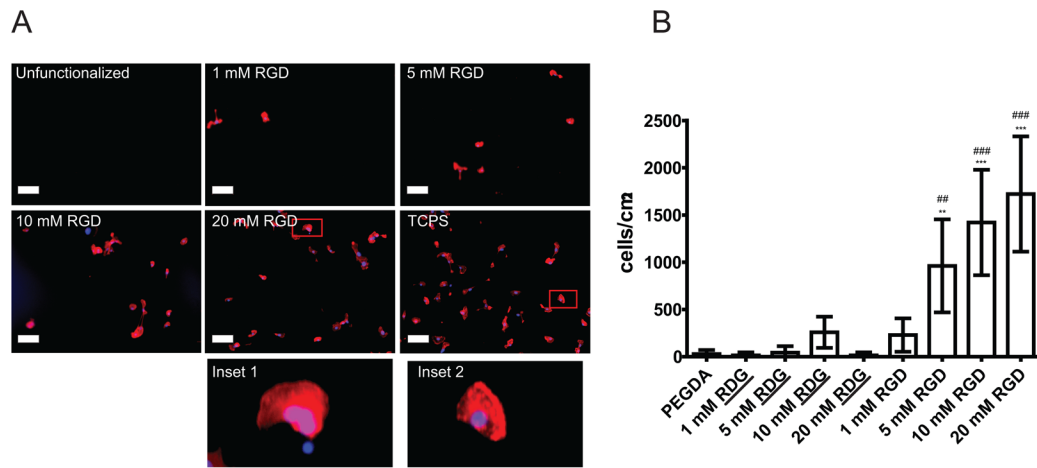




**Figure 2. Increasing molecular weight increases the swelling response of PEGDA hydrogels and decreases cell attachment**

A) Relaxed swelling ratio of PEGDA hydrogels with different molecular weight at different macromer concentrations in the initial solution. Swelling ratio increases with increasing molecular weight and increasing macromer concentration. No swelling is indicated by the dashed line, where  $Q_R = 1.0$ . Insert: AFM images of 4000 nm pitch topography showing the deformation of the topographic features in hydrogels due to swelling.

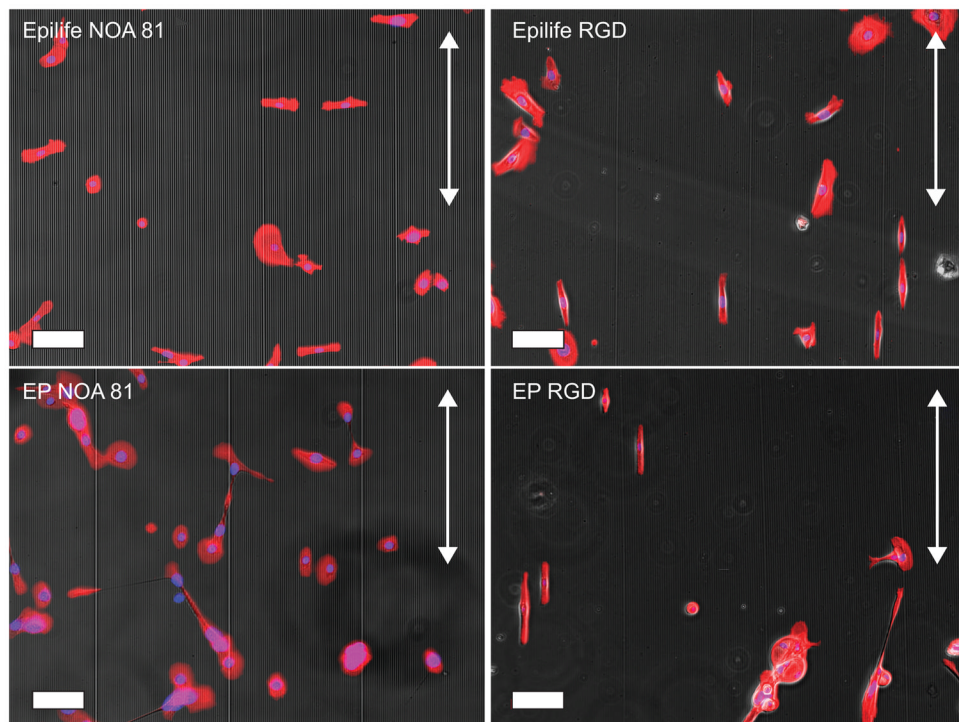
B) Cell attachment to unfunctionalized 20% (w/w) PEGDA hydrogels synthesized with macromers of molecular weight 700 g/mol and 3400 g/mol using EP media. PEGDA 3400 exhibits less non-specific cell attachment to the surfaces than PEGDA 700.



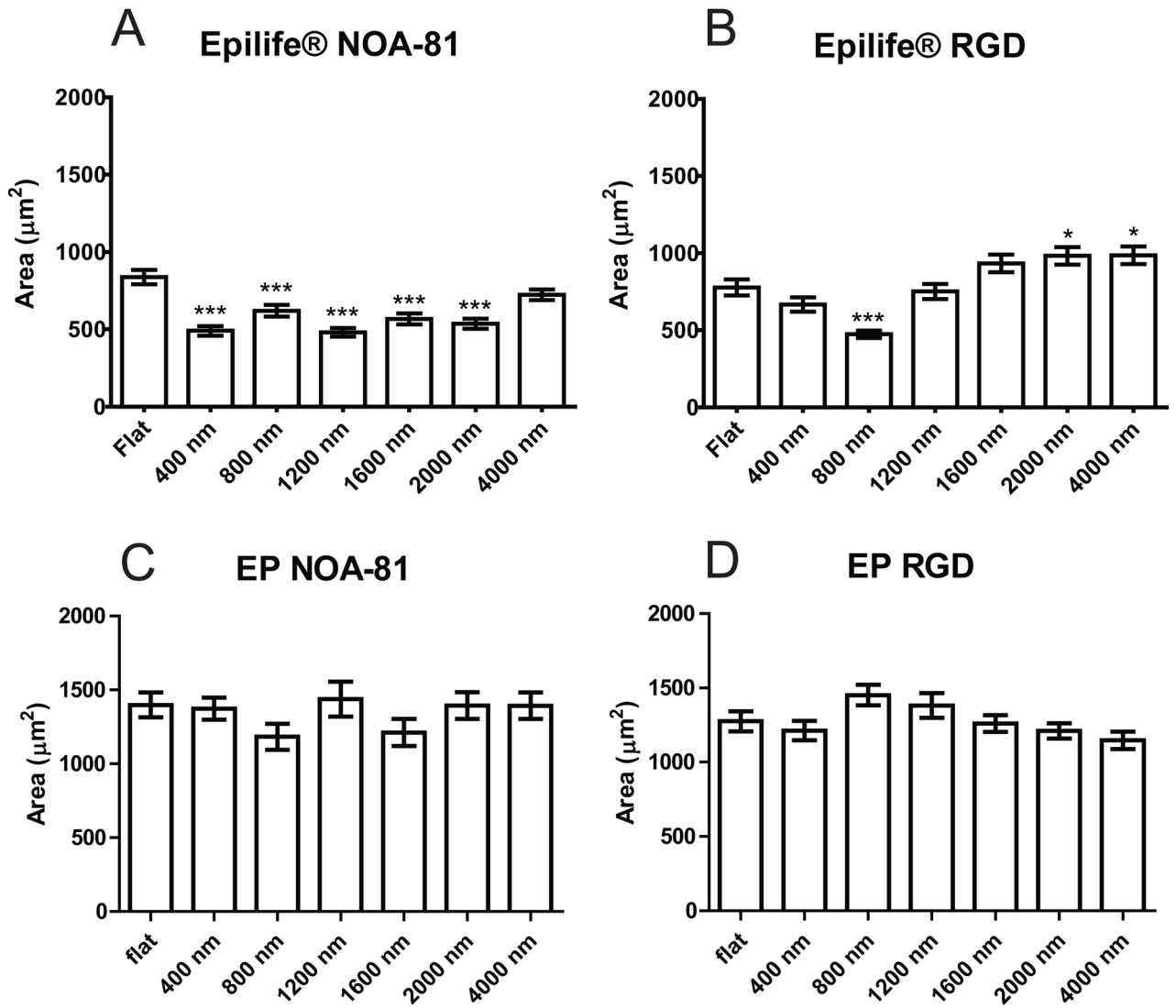
**Figure 3. Increasing the surface density of RGD promotes cell attachment**

A) Representative images demonstrating increasing levels of RGD peptide to promote cell attachment on PEGDA 3400/20% hydrogels. Cells were plated in EP media for 24 hours, followed by fixation, staining and analysis of cell attachment. Red: TRITC-Phalloidin. Blue: DAPI. Negative control: Unfunctionalized PEGDA. Positive control: Tissue Culture Polystyrene (TCPS). Scale bar: 100  $\mu$ m. Inset 1 (20 mM RGD surface) and inset 2 (TCPS) demonstrate similar cell spreading.

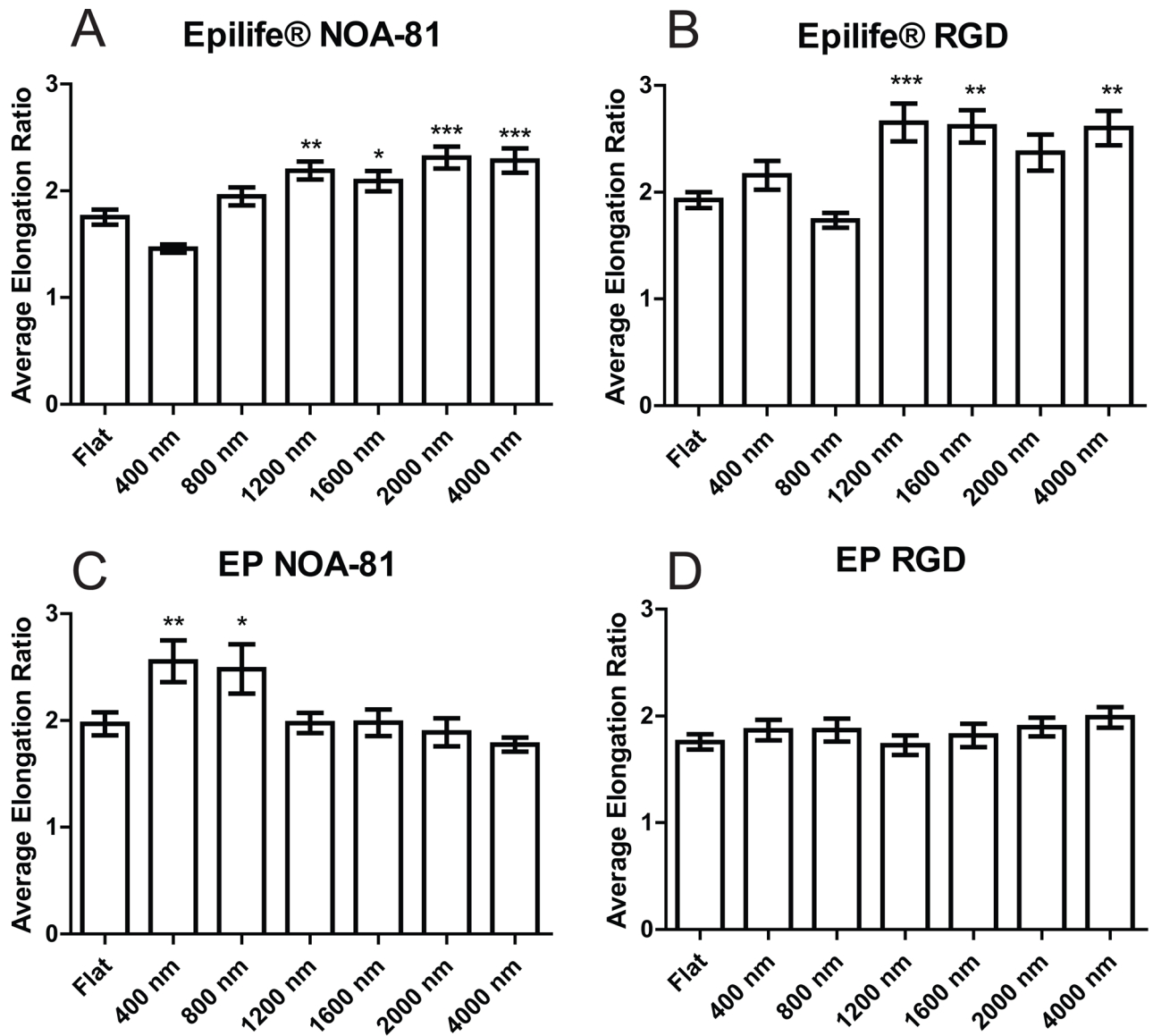
B) Cell attachment is RGD concentration dependent. In EP media, non-functionalized hydrogels made with PEGDA 3400/20% and hydrogels functionalized with scrambled peptide *RDG* presented no attachment of HCECs. Hydrogels functionalized with RGD had increased number of HCECs attached after 24-hours culture when the concentration of RGD increased. Error bars: SEM (\*: vs flat. #: vs scrambled. \*\*\* P 0.001; \*\* 0.001 < P 0.01; \* 0.01 < P 0.05).



**Figure 4.** HCECs cultured on 4000 nm pitch topography, using NOA-81 surfaces showed an alignment perpendicular to the topographic features in Epilife® medium, but perpendicular to the topography when cultured in EP medium. On RGD-functionalized hydrogels, the alignment is parallel to the topographic features regardless of media type. Arrows indicate the direction of the topographic features. Scale bar: 100  $\mu\text{m}$ .

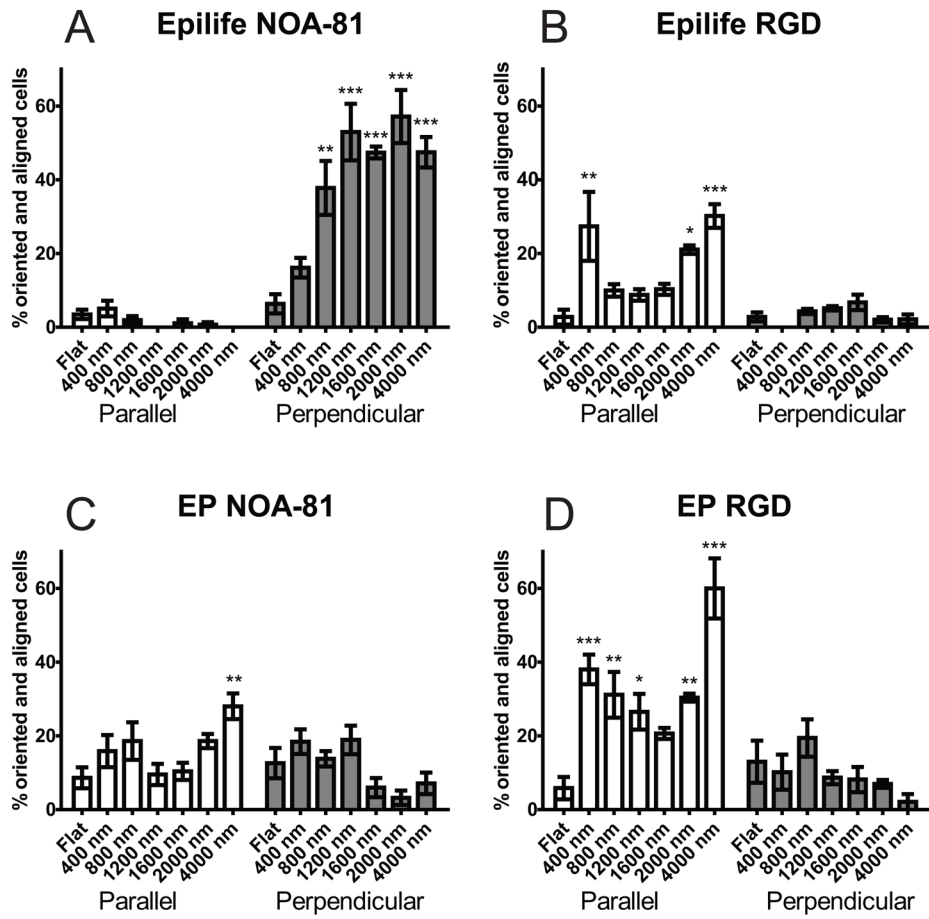


**Figure 5.** HCECs in Epilife® on NOA-81 were significantly smaller on the topographic surfaces than on flat surfaces, while HCECs in Epilife® on RGD hydrogels showed an increasing size with increasing topography. In EP medium, there was no significant difference for any type of substrate. A) Cells in Epilife® on NOA-81, B) Cells in Epilife® on RGD hydrogels, C) Cells in EP medium on NOA-81, D) Cells in EP medium on RGD hydrogels. Error bars: SEM (\*\*P 0.001; \*\* 0.001 < P 0.01; \* 0.01 < P 0.05).

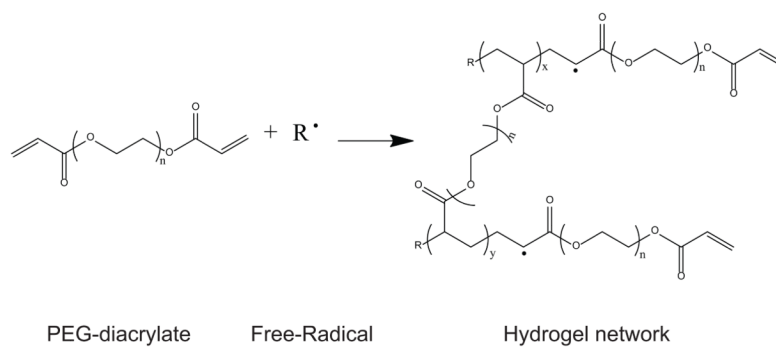
**Figure 6.**

HCECs in Epilife® on large-pitch topographic features (1200–4000 nm) showed a higher elongation ratio compared to flat surfaces on both types of substrates, NOA-81 and RGD hydrogels. HCECs in EP media showed no difference in elongation ratio with respect to planar on topographic features greater than 1200 nm. A) Cells in Epilife® on NOA-81, B) Cells in Epilife® on RGD hydrogels, C) Cells in EP medium on NOA-81, D) Cells in EP medium on RGD hydrogels. Error bars: SEM (\*\* $P < 0.001$ ; \*\*  $0.001 < P < 0.01$ ; \*  $0.01 < P < 0.05$ ).

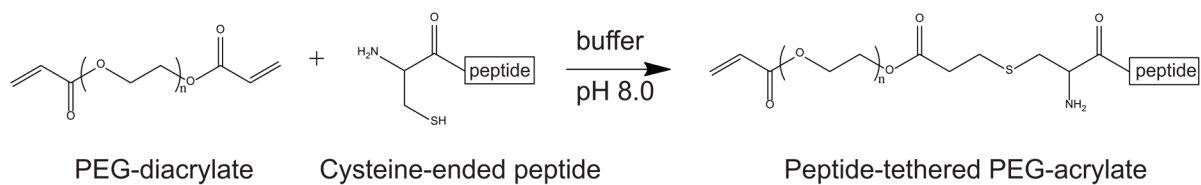




**Figure 7.** HCECs on NOA-81 surfaces showed an alignment behavior fundamentally different for the different media types. HCECs on RGD substrates showed the same alignment behavior for both media types. A) Cells in Epilife® on NOA-81, B) Cells in Epilife® on RGD hydrogels, C) Cells in EP medium on NOA-81, D) Cells in EP medium on RGD hydrogels. Error bars: SEM (\*\*P < 0.001; \*P < 0.05).

**Scheme 1.**

Free-radical polymerization of PEGDA for the formation of hydrogels. X and Y relate to the size of the poly(acrylate) domains. N relates to the size of the PEG domains

**Scheme 2.**

Michael-type addition reaction between a cysteine-containing peptide and PEGDA.

**Table I**

Molecular weight and mass fraction of the pre-polymer in the precursor solutions

Hydrogel Names	Molecular weight of PEGDApre-polymer	Mass fraction (w/w) in solution
P-700/10	700 g/mol	10%
P-700/15	700 g/mol	15%
P-700/20	700 g/mol	20%
P-700/25	700 g/mol	25%
P-700/40	700 g/mol	40%
P-3400/10	3400 g/mol	10%
P-3400/15	3400 g/mol	15%
P-3400/20	3400 g/mol	20%
P-3400/25	3400 g/mol	25%
P-8000/10	8000 g/mol	10%
P-8000/15	8000 g/mol	15%
P-8000/20	8000 g/mol	20%
P-8000/25	8000 g/mol	25%